Jurnal Rekayasa Mesin
p-ISSN: 1411-6863, e-ISSN: 2540-7678
Vol.21, No.2, August **2026**, p. 191-206

Analysis of The Effect of Fin Design Variations on Drag Coefficient and Drag Force on RX-450 Rocket Using CFD Simulation

Andi Wira Satria[1*], Edi Sofyan[2] and Muhammad Fa'iz Alfatih[3]
[1,2] Jurusan Teknik Dirgantara, Sekolah Tinggi Teknologi Kedirgantaraan,
Jl. Parangtritis No.5, Druwo, Bangunharjo, Kec. Sewon, Kabupaten Bantul, Daerah Istimewa Yogyakarta, 55187
[3] Jurusan Teknik Elektro, Sekolah Tinggi Teknologi Kedirgantaraan,
Jl. Parangtritis No.5, Druwo, Bangunharjo, Kec. Sewon, Kabupaten Bantul, Daerah Istimewa Yogyakarta, 55187
*E-mail: 21021583@students.sttkd.ac.id

Submitted: 03-12-2025; Accepted: 24-07-2026; Published: 31-08-2026

Abstract

Aerodynamic drag is one of the main factors affecting rocket performance during supersonic flight, as it directly influences stability, fuel efficiency, and flight range. This study was conducted to evaluate the influence of fin geometry variations specifically sweep angles (50°, 54.46°, and 60°) and semispan lengths (450 mm, 500 mm, and 550 mm) on the aerodynamic characteristics of the RX-450 rocket. The geometry was digitally modeled, and simulations based on Computational Fluid Dynamics (CFD) were carried out under airflow conditions at Mach 3.3. The results show that the fin design with a 60° sweep angle and 450 mm semispan yielded the lowest Coefficient of Drag (CD) and Drag Force (DF), at 0.0744 and 226.47 N, respectively. This design also fulfilled stability requirements, indicated by a positive stability margin. In conclusion, variations in fin design significantly affect the rocket's aerodynamic characteristics, and a smaller sweep angle with a shorter semispan is recommended to improve performance.

Keywords: *rocket; coefficient of drag; drag force; CFD simulation.*

Abstrak

Hambatan aerodinamika menjadi salah satu faktor penting yang memengaruhi kinerja roket pada kecepatan supersonik, karena berdampak langsung terhadap stabilitas penerbangan, efisiensi konsumsi bahan bakar, dan jarak tempuh roket. Penelitian ini dilakukan untuk mengevaluasi seberapa besar pengaruh perubahan geometri fin, khususnya sweep angle (50°, 54.46°, dan 60°) serta panjang semispan (450 mm, 500 mm, dan 550 mm), terhadap karakteristik aerodinamis roket RX-450. Pemodelan geometri dilakukan secara digital, dan simulasi berbasis Computational Fluid Dynamics (CFD) dijalankan pada kondisi aliran udara dengan kecepatan Mach 3.3. Hasil simulasi menunjukkan bahwa desain fin dengan sweep angle 60° dan semispan 450 mm menghasilkan nilai Coefficient of Drag (CD) dan Drag Force (DF) paling rendah, yaitu masing-masing sebesar 0.0744 dan 226.47 N. Desain ini juga memenuhi syarat stabilitas dengan nilai margin stabilitas yang positif. Kesimpulannya, variasi desain fin secara signifikan memengaruhi karakteristik aerodinamis roket, dan desain dengan sudut sweep kecil serta panjang semispan lebih pendek direkomendasikan untuk meningkatkan kinerjanya.

Kata kunci: roket; coefficient of drag; drag force; simulasi CFD.

1. Introduction

Rockets are vehicles that move on the principle of action-reaction and play an important role in a variety of applications, from satellite launches, space exploration, to defense systems. The development of rocket technology since World War II has resulted in significant improvements in the efficiency and reliability of launch systems. In the context of aerodynamic performance, one of the crucial aspects of rocket design is the fin tail, which functions to maintain stability and regulate the direction of the rocket during the flight phase [1].

Aerodynamics plays a major role in determining flight characteristics, such as fuel efficiency, flight stability, and range. Parameters such as Coefficient of Drag (CD) and Drag Force (DF) are important indicators in evaluating the aerodynamic efficiency of rockets. Properly designed fins can reduce air resistance and improve stability. In this case, fin geometry is a major factor that affects overall aerodynamic performance [2].

Copyright © 2026, https://jurnal.polines.ac.id/index.php/rekayasa

Various studies have been conducted to understand the effect of fin design on rocket performance. The results of the study show that fin shapes such as clipped delta and taper sweep are able to reduce drag at supersonic speeds [3]. In addition, analysis of the effect of fin shape on the static stability of sounding rockets indicates that fin geometry plays an important role in flight stability. Other studies have also revealed that the combination of nose cone and fin shape affects the directional stability and velocity of rockets [4,5]. In general, fin geometry variations have been shown to affect lift force, drag force, and the maximum height (apogee) reached by rockets [6,7]. However, no research has been found that specifically evaluates the fin design on the RX-450 rocket using a systematic Computational Fluid Dynamics (CFD)-based numerical approach.

The novelty of this study lies in the systematic investigation of the combined effects of sweep angle and fin semispan on the aerodynamic performance of the RX-450 rocket under supersonic conditions (Mach 3.3) using CFD simulation. Unlike previous studies that mainly focused on structural strength, flutter, or general fin-shape effects, this study provides a direct aerodynamic optimization of the RX-450 fin geometry based on Coefficient of Drag (CD), Drag Force (DF), and Stability Margin. The RX-450 rocket is a domestically produced two-stage rocket developed under the 2020–2024 National Research Priority (PRN) program, with a target altitude of more than 200 km. Although flight tests have been conducted, the aerodynamic performance of the RX-450 has not yet reached its target, with a maximum range of only 84 km. Previous studies have focused more on the structural aspects of the RX-450 fins, such as stress, flutter potential, and response to vibration [8-10], However, the effect of fin shape variations on the Coefficient of Drag (CD) and Drag Force (DF) has not yet been evaluated through CFD simulation.

This gap is the basis for this study. To date, there has been no comprehensive study evaluating the effect of variations in sweep angle and semi-span length of the RX-450 rocket fin on aerodynamic performance using CFD simulation. However, previous studies have shown that changes in fin design significantly affect the flow pattern and pressure distribution around the rocket body, which ultimately impacts overall aerodynamic efficiency [11,12]. The problem examined in this study is how fin design variations affect the Coefficient of Drag (CD) and Drag Force (DF) on the RX-450 rocket, and which fin design produces the lowest Coefficient of Drag (CD) and Drag Force (DF) values among the variations tested. To answer these questions, a CFD-based numerical simulation approach was used. The design variables that were varied included the sweep angle (50°, 54.46°, and 60°) and the semispan length (450 mm, 500 mm, and 550 mm). This study aims to determine the optimal design of the RX-450 fin in reducing Drag Force (DF) and improving aerodynamic efficiency. The results obtained are expected to contribute to the development of a more efficient national rocket design and can be used as a reference in the design of medium to high-range rockets. In addition, this study provides a scientific basis for the use of CFD methods to evaluate the aerodynamic performance of rocket components.

2. Material and Method

This study uses a quantitative approach based on numerical simulation to analyze the effect of fin design variations on the aerodynamic performance of the RX-450 rocket. This study is experimental in nature, with independent variables in the form of fin geometry variations, including leading edge sweep angle (50°, 54.46°, and 60°) and fin semispan length (450 mm, 500 mm, and 550 mm), resulting in nine design combinations, including the original design. The details of the design variations are presented in Table 1. The dependent variables observed were the Coefficient of Drag (CD) and Drag Force (DF) as the main indicators of aerodynamic performance. The overall research stages are illustrated in Figure 1.

Table 1. Fin design variation size

Design		Fin Semispan (mm)		
		450	**500**	**550**
	60	Variation 4	Variation 3	Variation 5
Sweep angle (°)	54.46	Variation 1	Original	Variation 2
	50	Variation 7	Variation 6	Variation 8

Figure 1. Research flowchart

The first stage in conducting the research was a literature study and problem identification to formulate design requirements and simulation parameters. After that, preliminary calculations are made to assess the stability of the rocket, which includes estimating the position of the center of gravity (CG), center of pressure (CP), and obtaining the Stability Margin value. These calculations are carried out in stages in the following order: determining the sweep angle on the mid-chord fin, calculating the length of the mid-chord fin, calculating the normal force on the nose cone, determining the position of the center of pressure on the nose cone, calculating the normal force on the four fins, calculating the interference factor for the four fins, calculating the normal force of the fins when interacting with the rocket body, determining the center of pressure on the fins, calculating the total normal force on the rocket, determining the position of the overall center of pressure of the rocket, calculating the center of gravity, and finally calculating the stability margin value (Equation (1)).

$$SM = \frac{(CP - CG)}{D} \quad (1)$$

Where: *SM* = static margin, *CP* = center of pressure (position from the tip of the nose cone), *CG* = center of gravity (position from the tip of the nose cone) and *D* = rocket diameter (450 mm).

The RX-450 rocket used in this study has a body diameter of 450 mm (0.45 m), which was used as the reference diameter in the Stability Margin calculation. Where the center of pressure can be calculated using the following Equation (2). Center of Gravity (CG) can be calculated using the following Equation (3).

$$\bar{X} = \frac{(C_{N\propto})_n \bar{X}_n + (C_{N\propto})_{fb} \bar{X}_f}{C_{N\propto}} \quad (2)$$

$$X_{CG}.W_{total} = (X_{CG_{nc}}.W_{nc}) + (X_{CG_{Body}}.W_{Body}) + (X_{CG_{Fin}}.W_{fin}.n) \quad (3)$$

Where : $\bar{X}$ = Pressure at a certain altitude (Pa), $(C_{N\propto})_n$ = Pressure at the lower boundary of the atmospheric layer (Pa), $\bar{X}_n$ = Temperature at the calculated altitude (K), $(C_{N\propto})_{fb}$ = Temperature at the lower boundary of the atmospheric layer (K), $\bar{X}_f$ = Center of pressure of Fin, $C_{N\propto}$ = Total normal force (Nosecone + Fin), X_{CG} = Center of gravity position of the nose cone tip, W_{total} = Total weight of the rocket, $X_{CG_{nc}}$= CG position of the nose cone, $X_{CG_{Body}}$ = CG position of the rocket body, $X_{CG_{Fin}}$= CG position of the rocket fins, W_{nc} = Weight of the nose cone, W_{Body} = Weight of the rocket body, W_{fin} = Weight of the rocket fins, and n = Number of fins.

If the calculation results show a positive value and indicate that the rocket is in a stable condition, the research process continues with the creation of a 3D design of the RX-450 rocket along with all fin variations. This 3D model covers the overall geometry of the rocket with each fin variation that has been designed. The details of the RX-450 rocket geometry and all fin variations are presented in Table 2.

Table 2. RX-450 Rocket Design and Fin Variations

Design	Image
RX-450 rocket design	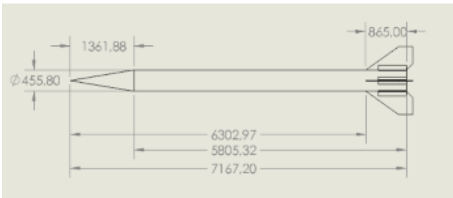
Original fin design	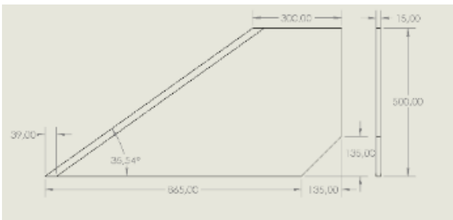
Variation 1 fin design	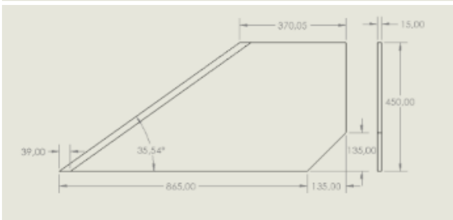

Design	Image
Variation 2 fin design	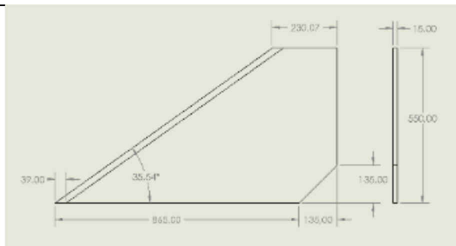
Variation 3 fin design	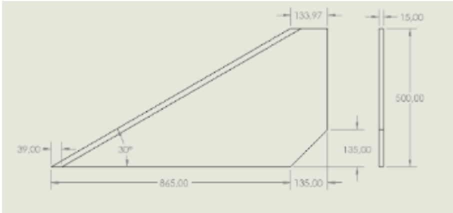
Variation 4 fin design	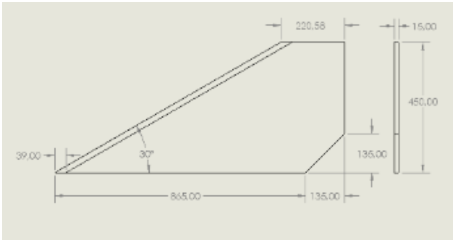
Variation 5 fin design	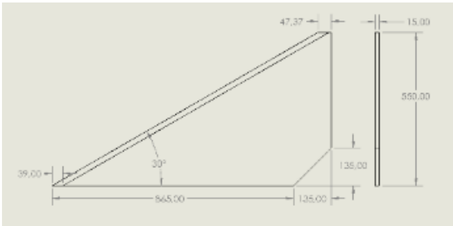
Variation 6 fin design	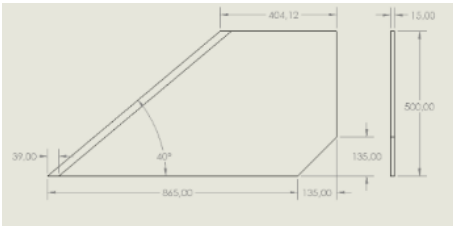
Variation 7 fin design	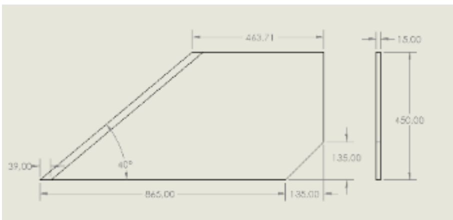
Variation 8 fin design	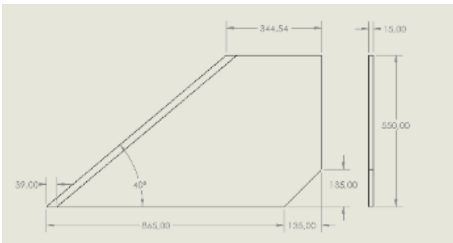

The resulting design model is then entered into the simulation environment and placed in a fluid domain that has been cut into quarters for computational efficiency. The next process is mesh generation, which involves dividing the fluid domain into small elements. A denser mesh is used around the rocket through a local sizing technique to improve the accuracy of the results, while the outer area is made coarser to speed up the simulation time. The specific meshing parameters used in this study are listed in Table 3. The quality of the mesh is validated using parameters such as skewness and orthogonal quality, with threshold values adjusted to ensure accurate simulation results.

Table 3. Meshing Input

No	Parameter	Option/Value
Add Local Sizing		
1	Body Of Influence	0.04
2	Growth Rate	1.2
Generate the Surface Mesh		
1	Minimum Size	0.01
2	Maximum Size	0.6
3	Growth Rate	1.2
4	Size Functions	Curvature & Proximity
5	Curvature Normal Angle	18
6	Cells Per Gap	1
7	Scope Proximity To	Edges
Describe Geometry		
1	Geometry Type	The geometry consist of only fluid regions with no voids
Add Boundary Layers		
1	Uniform	0.001
2	Number of Layers	5
3	Growth Rate	1.2
4	Add in	fluid-regions
5	Grow on	only-walls
Generate the Volume Mesh		
1	Solver	Fluent
2	Fill With	poly-hexcore
3	Peel Layers	1
4	min Cell Length	0.01
5	Max Cell Length	0.32

CFD simulations were performed under compressible supersonic airflow conditions at a Mach number of 3.3. The turbulence model used was k-ω SST, which is suitable for handling high pressure gradients and complex geometries. The fluid used was air with thermophysical properties referring to the ideal gas model and Sutherland's law for viscosity. Reference values such as velocity, density, pressure, and cross-sectional area were adjusted to the actual flight conditions of the rocket. The Y+ value used for the heat transfer coefficient in this simulation was set to 300 (Table 5), corresponding to the use of standard/scalable wall functions to model the near-wall region rather than fully resolving the viscous sublayer, which would require Y+ close to 1. Because the drag values of interest (CD and DF) are dominated by pressure drag arising from the supersonic shock structure around the fins and body rather than by fine-scale near-wall shear alone, a wall-function treatment with Y+ ≈ 300 is commonly regarded as adequate for capturing the overall force coefficients under the k-ω SST model, although it does not fully resolve boundary-layer separation details. Future studies are encouraged to verify this assumption using a low-Reynolds-number near-wall treatment with Y+ ≈ 1 and additional inflation layers. The density and viscosity can be calculate using Equation 4 and 5.

$$\rho = \frac{P}{RT} \quad (4)$$

$$\mu = \mu_0 \left(\frac{T}{T_0}\right)^{3/2} \cdot \frac{T_0 + S}{T + S} \quad (5)$$

Where : P is air pressure at a certain altitude (Pascal), R is specific gas constant for dry air (287 J/(kg.K)), T is air temperature at a certain altitude (K), μ is Dynamic viscosity, μ_0 is Reference viscosity at T_0, T is Actual temperature, T_0 is Reference temperature, S is sutherland constant.

The air material properties used in the simulation are presented in Table 4. The reference values for the boundary conditions of each design variation are listed in Table 5.

Table 4. Air Material Property Input

Property	Value	Data Type
Density	Ideal Gas	ideal-gas
Specific Heat Cp	1004.67	constant
Thermal Conductivity	0.0242	constant
Viscosity	sutherland	sutherland
Molecular Weight	28.966	constant

The air properties used in the simulation were obtained based on the atmospheric conditions at a certain altitude using the International Standard Atmosphere (ISA) model. These properties were calculated using several governing equations. The specific enthalpy, atmospheric pressure, and air temperature were calculated using Equations (6) to (8). Meanwhile, the flow velocity and speed of sound were calculated using Equations (9) and (10).

$$h = c_p \times T \tag{6}$$

Where : h = Specific enthalpy (J/kg), c_p = Specific heat at constant pressure (J/kg·K), and T = Temperature (K).

$$P = P_b . \left(\frac{T}{T_b}\right)^{-\frac{g}{R.L}} \tag{7}$$

Where : P = Pressure at a certain altitude (Pa), P_b = Pressure at the lower boundary of the atmospheric layer (Pa), T = Temperature at the calculated altitude (K), T_b = Temperature at the lower boundary of the atmospheric layer (K), g = Acceleration due to gravity (9.80665 m/s²), R = Gas constant (8.31432 J/(mol·K)), and L = Lapse rate (0.001 K/m).

$$T = T_0 + L \times (h - h_0) \tag{8}$$

Where : T = Temperature at altitude h (K), T_0 = Reference temperature at altitude h0 (K), L = Lapse rate (0.001 K/m), h = Altitude (m), and h_0 = Lower boundary of layer (m).

$$v = M.a \tag{9}$$

Where : v = Velocity (m/s), M = Mach number, and a = Speed of sound in the atmosphere (m/s).

$$a = \sqrt{\gamma R T} \tag{10}$$

Where : a = Speed of sound in the atmosphere (m/s), γ = Specific heat ratio of air (1.4 for dry air), R = Specific gas constant for dry air (287 J/(kg·K)), and T = Air temperature at a certain altitude (K).

Table 5. Reference Value Input

Parameter	Value (Design Type)		
	V1, V4, V7	Asli, V3, V6	V2, V5, V8
Compute From		Inlet	
Area [m²]	0.190172	0.193172	0.196172
Density [kg/m³]		0.0328	
Enthalpy [J/kg]		224026	
Length [m]		7.1672	
Pressure [Pa]		2101.5	
Temperature [K]		223.10	
Velocity [m/s]		987.99	
Viscosity [kg/(m·s)]		1.455e-05	
Ratio of Specific Heats (γ)		1.4	
Yplus for Heat Transfer Coeff		300	
Reference Zone		Enclosure	

After all settings are complete, the initialization process is carried out to accelerate convergence, then continued with simulation until reaching 1000 iterations or numerical convergence. The Drag Coefficient (CD) and Drag Force (DF) values are monitored through report definitions and residual monitors. After the simulation is complete, the results are evaluated for aerodynamic coefficient values. The results of each design variation were compared to determine the most optimal fin configuration. The analysis also included rechecking the stability margin values to ensure that the design with the lowest drag still met the stability criteria. With a combination of aerodynamic efficiency and stability, a fin design was obtained that can be recommended for further development of the RX-450 rocket.

3. Results and Discussion

3.1 Stability Margin

The calculated values of the Center of Pressure (CP) and Center of Gravity (CG) for all design variations are presented in Table 6, and the corresponding stability margin values are illustrated in Figure 2.

Table 6. Center of Pressure and Center of Gravity Values

Design Type	Center of Pressure (mm)	Center of Gravity
Original	5827.37	5371.57
Variation 1	5687.69	5231.89
Variation 2	5935.97	5480.17
Variation 3	5790.28	5334.48
Variation 4	5663.49	5207.69
Variation 5	5881.69	5425.89
Variation 6	5834.54	5378.74
Variation 7	5691.04	5235.24
Variation 8	5948.28	5492.48

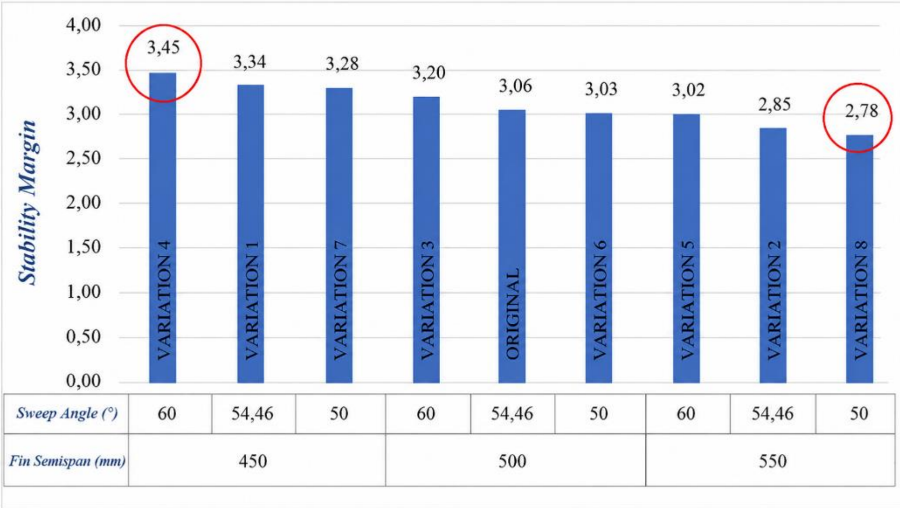

Figure 2. Stability Margin value graph against design

From the table above, all configuration variations show stability margin values of more than 2 calibers, which means that all designs fall into the longitudinally stable category. However, the design with the highest Stability Margin is Variation 4 (3.45), while the lowest is Variation 8 (2.77). The original design is at 3.06, which is still within the stable range. All design variations continue to meet the safety stability criteria for flight.

3.2 Mesh Quality

Table 7. Mesh Quality

Design	Total Cell	Skewness Quality		Orthogonal Quality	
		Value	Quality	Value	Quality
Original	796693	0.73	Good	0.20	Good
Variation 1	834669	0.74	Good	0.20	Good
Variation 2	796725	0.71	Good	0.20	Good
Variation 3	794020	0.74	Good	0.22	Good
Variation 4	757961	0.71	Good	0.23	Good
Variation 5	854991	0.71	Good	0.22	Good
Variation 6	798746	0.71	Good	0.21	Good
Variation 7	799014	0.75	Good	0.23	Good
Variation 8	761654	0.72	Good	0.21	Good

Table 7 summarizes the mesh quality metrics obtained for all nine design variations. The skewness values range from 0.71 to 0.75, while the orthogonal quality values range from 0.20 to 0.23, both metrics fall within the "Good" category based on standard ANSYS Meshing quality criteria, in which skewness values approaching 0 and orthogonal quality values approaching 1 indicate a well-formed, non-distorted mesh. The total cell count ranges from 757.961 cells (Variation 4) to 854.991 cells (Variation 5), with the difference in cell count reflecting the difference in fin surface area and semispan length among the geometries. Because all variations produced skewness and orthogonal quality values within the recommended "Good" range, and the boundary-layer and local-sizing settings (Section 2) were kept identical across variations, the resulting meshes are considered sufficiently regular and orthogonal to support numerically stable and reliable CFD computations for all nine configurations.

p-ISSN: 1411-6863, e-ISSN: 2540-7678
Vol.21|No.2|191-206|August|2026

Although a formal Grid Convergence Index (GCI) study was not performed in this work, several considerations support the adequacy of the approximately 800.000-cell mesh used for all variations. First, the mesh density was not selected arbitrarily: an identical local-sizing strategy was applied to every variation, using a Body of Influence growth factor of 0.04, curvature-based surface sizing (minimum 0.01 m, maximum 0.6 m), and five inflation layers with a first-layer height of 0.001 m and a growth rate of 1.2 (Table 3), concentrating cells near the fin and body surfaces where velocity and pressure gradients are steepest under Mach 3.3 flow. Second, the resulting skewness (0.71-0.75) and orthogonal quality (0.20-0.23) values (Table 7) remained within the "Good" range for all nine geometries despite the approximately 100.000-cell variation in total cell count driven by differences in fin surface area, indicating consistent mesh quality across the design space. Third, because the same meshing strategy, boundary-layer settings, and solver settings were applied consistently to every variation, the relative comparison between fin designs is expected to be considerably less sensitive to the absolute cell count than the absolute CD and CF values would be. Nevertheless, these arguments do not substitute for a formal mesh-independence study. Future extensions of this work should perform a systematic grid-refinement study (e.g., using Roache's GCI method with coarse, medium, and fine meshes) to quantify the discretization uncertainty in the reported CD and CF values.

3.3 Contour Visualization

Table 8. Contour Pressure

Desain	Contour Pressure
Original	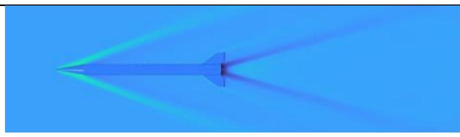
Variation 1	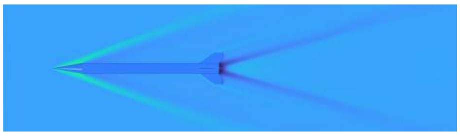
Variation 2	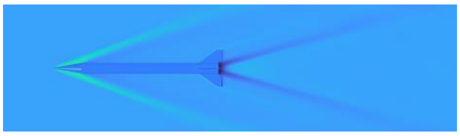
Variation 3	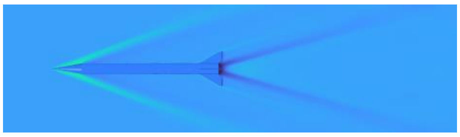
Variation 4	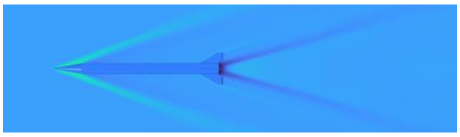
Variation 5	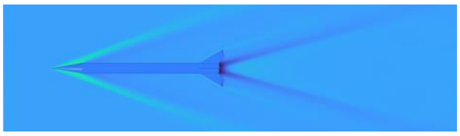

Desain	Contour Pressure
Variation 6	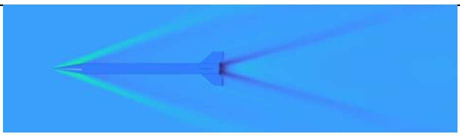
Variation 7	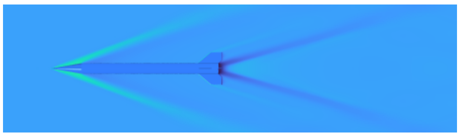
Variation 8	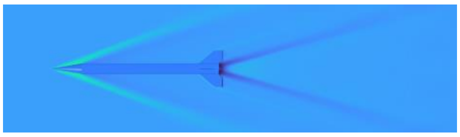

The pressure contour (Table 8) illustrates the pressure distribution around the RX-450 rocket for each fin configuration. The highest pressure occurs at the nose cone due to the stagnation effect under supersonic flow conditions, while pressure variations are mainly observed around the fin and aft-body region. The low-pressure area behind the fin indicates the formation of a wake region associated with pressure drag, suggesting that fin geometry influences the aerodynamic drag characteristics of the rocket.

Table 9. Contour Velocity

Design	Contour Velocity
Original	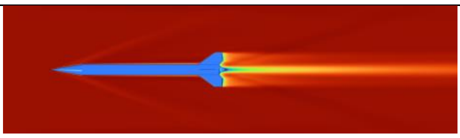
Variation 1	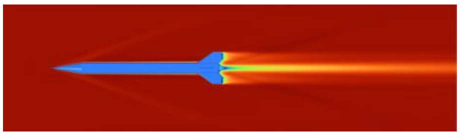
Variation 2	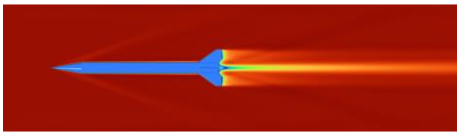
Variation 3	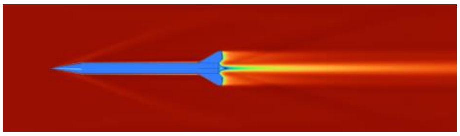
Variation 4	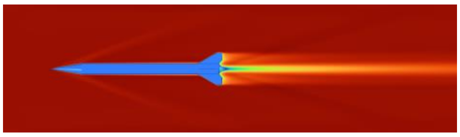
Variation 5	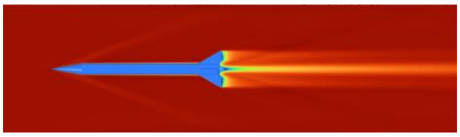

Design	Contour Velocity
Variation 6	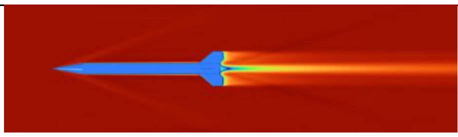
Variation 7	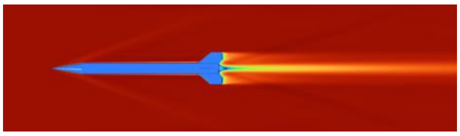
Variation 8	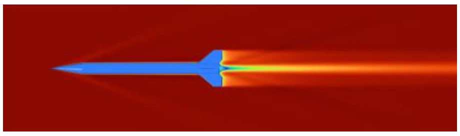

The velocity contour (Table 9) shows that the airflow decelerates at the nose cone due to the stagnation region and remains attached along the rocket body. Slight differences appear around the fin and wake region, where low-velocity zones are formed downstream of the fin. A narrower wake region indicates lower momentum loss and reduced aerodynamic drag, whereas a wider wake suggests stronger flow separation and higher drag.

3.4 Simulation Results of Drag Coefficient and Drag Force (N)

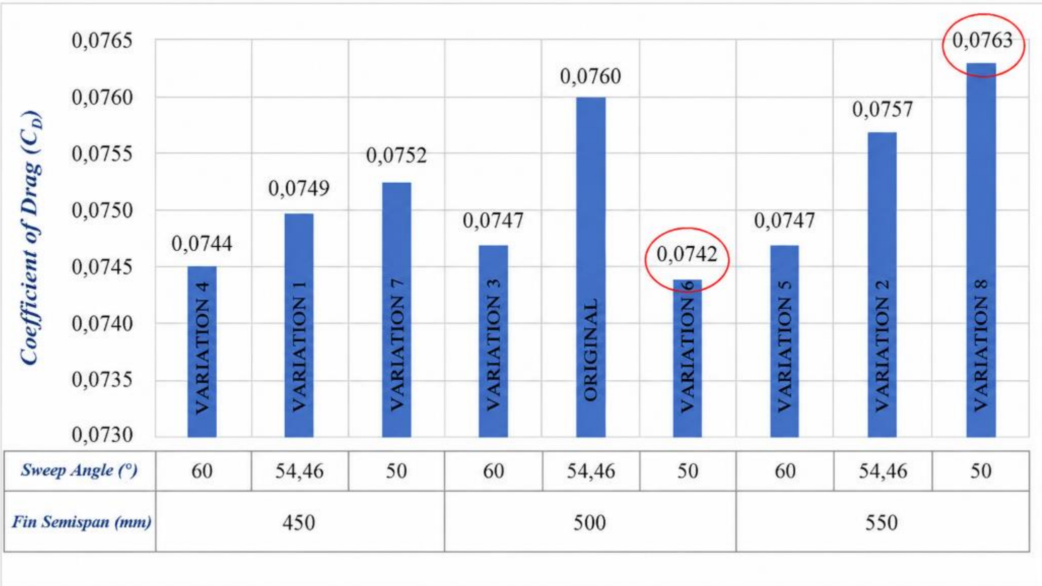

Figure 3. Comparison chart of Coefficient of Drag with design

From the graph (Figure 3), variation 6 produced the lowest Coefficient of Drag value of 0.0742. This was followed by variation 4 (0.0744), variations 3 and 5 (both 0.0747), and variation 1 (0.0749). Meanwhile, variations 2 and 7 have Coefficient of Drag values of 0.0757 and 0.0752, respectively. The original design has a Coefficient of Drag value of 0.0760. The highest Coefficient of Drag value is obtained in variation 8, which is 0.0763.

Based on the graph (Figure 4), variation 4 has the lowest Drag Force value of 226.47 N, followed by variation 1 (228.30 N), variation 7 (228.86 N), and variation 6 (229.41 N). The highest Drag Force value was found in variation 8 with 239.71 N, followed by variation 2 (237.99 N) and variation 5 (234.57 N). The original rocket design had a value of 235.26 N, while variation 3 recorded a value of 231.15 N.

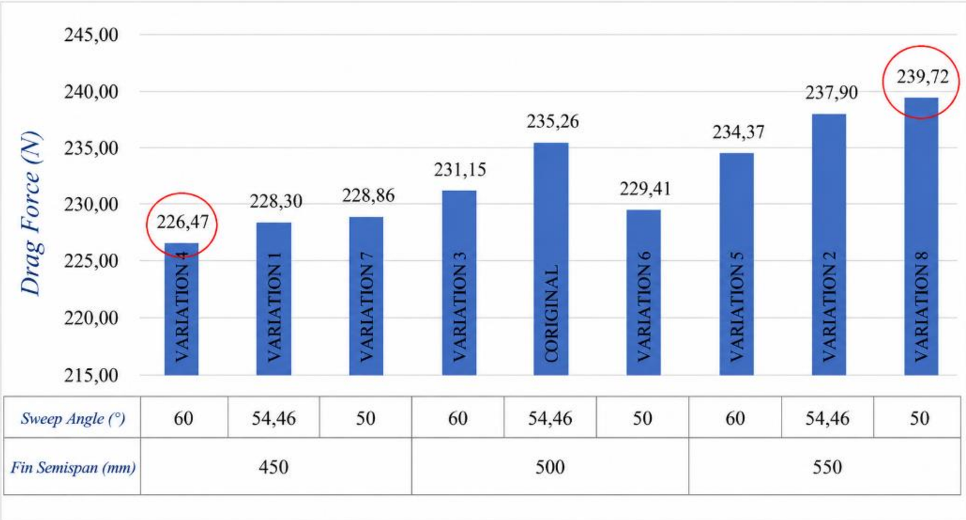

Figure 4. Comparison graph of Drag Force (N) with design

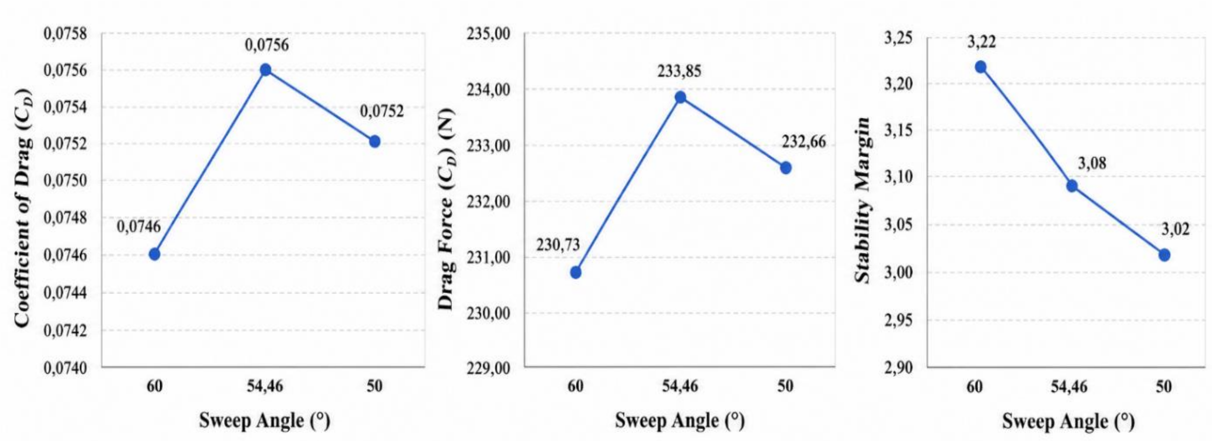

Figure 5. Comparison graph of Sweep Angle (°) with Coefficient of Drag (CD), Drag Force (DF), and Stability Margin

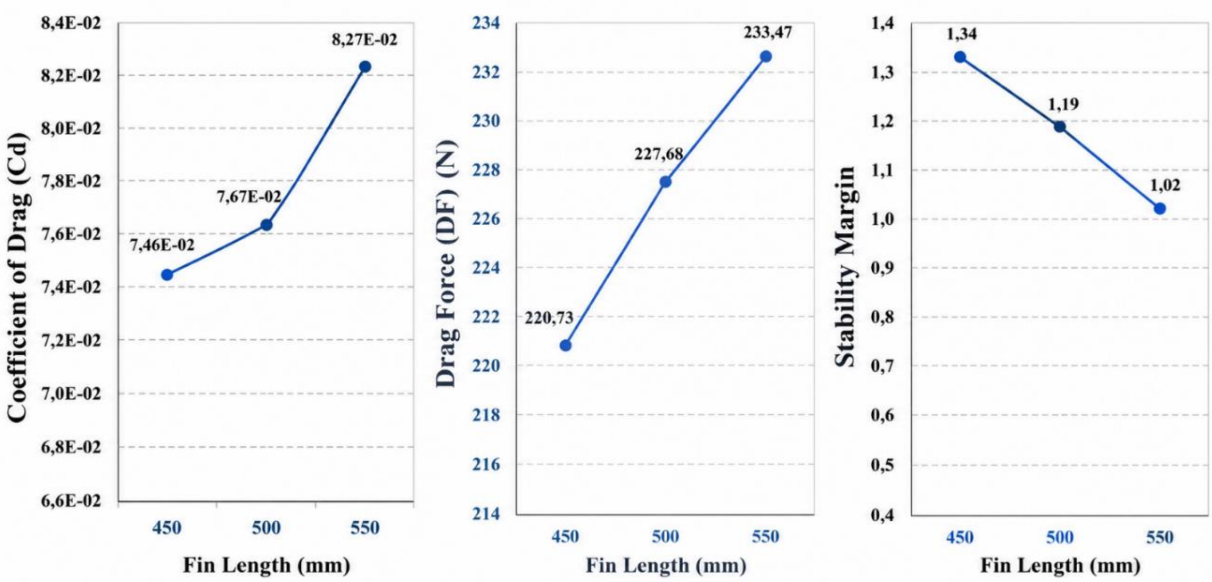

Figure 6. Comparison chart of fin semispan with Coefficient of Drag (CD), Drag Force (DF), and Stability Margin

Based on the simulation results (Figure 5), variations in sweep angle have a significant effect on the aerodynamic characteristics of the RX-450 rocket. At a sweep angle of 60°, the lowest Coefficient of Drag (CD) value of 0.0746, the lowest Drag Force of 230.73 N, and the highest Stability Margin of 3.22 were obtained. Conversely, a sweep angle of 54.46° resulted in the highest Drag Coefficient (CD) and Drag Force (DF) values, at 0.0756 and 233.85 N, respectively, with a lower stability margin value. Meanwhile, a sweep angle of 50° showed values between the two. This pattern shows that a larger sweep angle tends to reduce Drag Force (DF) and increase rocket stability. Therefore, a fin configuration with a sweep angle of 60° can be considered the most appropriate choice in the context of the RX-450 rocket's aerodynamics.

Based on the simulation results (Figure 6), increasing the length of the semispan fin affects the aerodynamic parameters of the RX-450 rocket. The Coefficient of Drag (CD) value increased from 0.0749 at a semispan of 450 mm to 0.0756 at 550 mm, along with an increase in Drag Force from 227.88 N to 237.43 N. This shows that the greater the surface area of the fin in contact with the airflow, the greater the Drag Force (DF) produced. On the other hand, the Stability Margin decreased from 3.36 to 2.88, indicating that a longer semispan tends to shift the Center of Pressure closer to the Center of Gravity, thereby reducing the rocket's static stability. Therefore, the selection of the semispan length needs to consider the balance between air resistance and stability.

3.5 Discussion

The results of this study indicate that fin design variations have a significant impact on the Coefficient of Drag (CD) and Drag Force (DF) values of the RX-450 rocket. This is in line with aerodynamic theory, which states that fin geometry affects the flow and pressure distribution around the rocket body. The decrease in the Coefficient of Drag (CD) value in several designs supports previous findings which concluded that a combination of optimal sweep angle and appropriate fin surface area can reduce Drag Force (DF) [13], which found that fin drag increases approximately linearly with fin semispan for a low-altitude rocket configuration. This trend is quantitatively confirmed by the present results: increasing the semispan from 450 mm to 550 mm raised the CD of the RX-450 fin from 0.0749 to 0.0756 (a 0.9% increase) and the DF from 227.88 N to 237.43 N (a 4.2% increase), consistent in direction with the near-linear semispan-drag relationship reported in [13], although the absolute CD and DF values are not directly comparable because the two studies use different rocket geometries, diameters, and flight Mach numbers.

These findings are also consistent with studies emphasizing the importance of the geometric configuration of the rear section of the rocket in improving stability and reducing drag [14], whose CFD and semi-empirical (USAF DATCOM) analysis of a curved-fin sounding rocket reported that both the normal-force and drag coefficients increase with angle of attack and with Mach number. A directly analogous trend is observed in the present study for sweep angle: reducing the sweep angle from 60° to 54.46° increased CD by 1.3% (from 0.0746 to 0.0756) and DF by 1.3% (from 230.73 N to 233.85 N), while decreasing the Stability Margin, showing that both fin sweep and semispan variations shift the balance between drag and stability in a manner consistent with the flow-sensitivity trends reported in that study.

Other studies further show that curved-fin designs can produce lower Coefficient of Drag (CD) than conventional straight/swept shapes [15]. In quantitative terms, the best-performing configuration identified in this study, Variation 4 (60° sweep angle, 450 mm semispan), reduced Coefficient of Drag (CD) by 2.1% (from 0.0760 to 0.0744) and Drag Force (DF), by 3.7% (from 235.26 N to 226.47 N) relative to the original RX-450 fin design, while still increasing the Stability Margin from 3.06 to 3.45 calibers. This combination of reduced drag and improved stability for a straight, swept fin geometry is directionally consistent with the drag-reduction magnitudes reported for optimized fin configurations in [13]-[15], although a direct percentage-for-percentage comparison with those studies is not meaningful because they were conducted on different rocket bodies, fin baselines, and flow regimes (subsonic-to-transonic Mach 0.6-1.2 in [15] versus supersonic Mach 3.3 in the present study). In addition, other reviews state that fin configuration optimization is an effective strategy for reducing drag and improving stability, especially in small satellite launch vehicles.

The CFD simulation approach used in this study is also in line with design evaluation methods that have been widely applied in aerodynamic studies [16]. Thus, the results of this study reinforce that choosing the right fin design plays an important role in reducing drag and maintaining rocket stability, especially at high speeds.

4. Conclusion

Based on the results of CFD simulations and Stability Margin calculations that have been carried out on eight variations of the RX-450 rocket fin design, it can be concluded that variations in fin shape and size have a significant effect on the Coefficient of Drag (Cd) and Drag Force (DF) values. Fin designs with a small sweep angle and shorter semispan tend to produce lower Drag Force (DF), indicating that fin geometry directly affects the aerodynamic performance of the rocket. Among all the variations tested, Variation 4 showed the most optimal results with the lowest Coefficient of Drag (CD) and Drag Force (DF) values, namely 0.0744 and 226.47 N. This indicates that this fin design has the most aerodynamic shape characteristics compared to other variations for flight conditions at Mach 3.3.

For further research, it is recommended to conduct direct flight tests on the analyzed fin design to validate the CFD simulation results under operational conditions. In addition, it is advisable to use actual material models on the rocket geometry to take into account thermal and structural loads, as well as to perform simulations at various Mach numbers to evaluate the fin design's response to varying flight conditions. Further research should also consider the influence of Center of Pressure (CP) and Center of Gravity (CG) dynamics during the flight phase to support a comprehensive analysis of rocket stability.

Acknowledgement

The author would like to thank the Yogyakarta College of Aerospace Technology (STTKD) for the facilities and academic support provided during this research process. Thanks are also extended to the supervising lecturer for the guidance and input that were invaluable in the implementation and preparation of this research.

References

[1] P. Tseung, “Innovation in Hybrid Rocket Propulsion System,” Int. J. Multidiscip. Innov. Res. Methodol. ISSN 2960-2068, vol. 1, no. 1, hal. 1–7, 2022.

[2] S. Umarani, “Synergy of Aerodynamics and Propulsion: A Comparative Study in Flight and Rocketry,” Int. J. Multidiscip. Res. E-ISSN 2582-2160, vol. 6, no. 4, hal. 26, 2024.

[3] K. Ukirde, S. Pawar, D. Rahane, B. Sagar, dan T. Shinde, “Aerodynamic Study of Various Fins for Missile Body,” Int. J. Res. Appl. Sci. Eng. Technol., vol. 11, no. 2, hal. 1240–1252, 2023, doi: 10.22214/ijraset.2023.49235.

[4] A. Schoch, “Rocket stability assessment: CFD analysis of fin shapes and their impact on the static stability of a sounding rocket,” 2023.

[5] M. A. Abdul Hamid, A.H., Salleh, Z., Muhammad, M.A., Kamaludin, K., Sujana, M.J., and Khamis, “The Effect of Different Designs of Fins and Nose Cones towards the Stability and Performance of a Sugar Rocket,” Int. Trans. J. Eng. Manag. Appl. Sci. Technol., vol. 13, no. 13, hal. 1–15, 2022, doi: 10.14456/ITJEMAST.2022.262.

[6] M. H. Shahir dan A. Sapit, “A Study On Aerodynamic Shape of Fin of Model Rocket using Computational Fluid Dynamics (CFD),” Res. Prog. Mech. Manuf. Eng., vol. 2, no. 2, hal. 988–996, 2021.

[7] A. Pektaş, Z. Demircan, Ü. Hacıabdullahoğlu, N. Ejder, dan C. Tola, "Effects of different fin shapes on apogee and stability of model rockets," in 2019 9th International conference on recent advances in space technologies (RAST), IEEE, 2019, hal. 193–199.

[8] G. Ronald, D. A. Budi, W. Bagus, dan A. Haryadi, "Strength Design of Rx 450 Rocket Fin Due To Effect of Aerodynamic Load," Innov. Res. Sci. Technol. Cult., hal. C13–C19, 2020.

[9] A. B. Djatmiko, "Perancangan Sirip Roket RX 450 Akibat Pengaruh Terjadinya Flutter," 2021.

[10] D. A. Budi, R. Fauzhia, dan B. G. Yuniati Erma, "Perancangan kekuatan sirip roket RX 450 seri 18.01 akibat pengaruh beban getaran," J. Tek. Kim., vol. 27, no. 3, hal. 88–94, 2021.

[11] Le, Vu & Nguyen, Anh Tuan & Nguyen, Lac & Dang, Ngoc & Tran, Ngoc-Doan & Han, Jae-Hung. (2021). Effectiveness Analysis of Spin Motion in Reducing Dispersion of Sounding Rocket Flight due to Thrust Misalignment. International Journal of Aeronautical and Space Sciences. 22. 10.1007/s42405-021-00383-x.

[12] D. Panchigar, K. Kar, S. Shukla, R. M. Mathew, U. Chadha, dan S. K. Selvaraj, "Machine learning-based CFD simulations: a review, models, open threats, and future tactics," Neural Comput. Appl., vol. 34, no. 24, hal. 21677–21700, 2022.

[13] A. A. Adnan, A. H. Abdul Hamid, Z. Salleh, dan M. Z. Azizi, "Mathematical and Computational Fluid Dynamics Analysis of Low-Altitude Rocket Drag for Various Fin Configurations," 2024. doi: 10.6125/JoAAA.202407_56(3).12.

[14] N. Dahalan, A. F. Suni, I. Ishak, N. A. R. Nik Mohd, dan S. Mat, "Aerodynamic study of air flow over a curved fin rocket," J. Adv. Res. Fluid Mech. Therm. Sci., vol. 40, hal. 46–58, Des 2017.

[15] Barokah, Arief & Sabino, Ubaidillah & Lenggana, Bhre & Wibawa, Lasinta & Kusumandari, Dwi & Joelianto, Endra & Hoa, Nguyen. (2024). A Comparative Analysis of Aerodynamic Performance: Straight Fin and Curved Fin Rockets using Computational Fluid Dynamics (CFD). Journal of Advanced Research in Fluid Mechanics and Thermal Sciences. 115. 1-18. 10.37934/arfmts.115.1.118.

[16] S. Sankalp, V. Sharma, A. Singh, A. Salian, dan G. Srinivas, "Computational analyses of tail fin configurations for a sounding rocket," Aerosp. Syst., vol. 5, Nov 2021, doi: 10.1007/s42401-021-00116-8.